scientific reports

Check for updates

OPEN

Microscopy and spatial-metabolomics identify tissue-specific metabolic pathways uncovering salinity and drought tolerance mechanisms in *Avicennia marina* and *Phoenix dactylifera* roots

Paula Oyarce[1], Ting Ting Xiao[1], Corinna Henkel[2], Signe Frost Frederiksen[3], Jose Kenyi Gonzalez-Kise[1], Wouter Smet[1], Jian You Wang[4], Salim Al-Babili[4] & Ikram Blilou[1]✉

In arid and semi-arid climates, native plants have developed unique strategies to survive challenging conditions. These adaptations often rely on molecular pathways that shape plant architecture to enhance their resilience. Date palms (*Phoenix dactylifera)* and mangroves (*Avicennia marina)* endure extreme heat and high salinity, yet the metabolic pathways underlying this resilience remain underexplored. Here, we integrate tissue imaging with spatial metabolomics to uncover shared and distinct adaptive features in these species. We found that mangrove roots accumulate suberin and lignin in meristematic tissues, this is unlike other plant species, where only the differentiation zones contain these compounds. Our metabolomic analysis shows that date palm roots are enriched in metabolites involved in amino acid biosynthesis, whereas compounds involved in lignin and suberin production were more abundant in mangrove roots. Matrix-assisted laser desorption/ionization mass spectrometry imaging (MALDI-MSI) revealed tissue- and species-specific metabolite distributions in root tissues. We identified common osmoprotectants accumulating in the exodermis/epidermis of date palm and mangrove root meristems, along with a unique metabolite highly abundant in the inner cortex of date palm roots. These findings provide valuable insights into stress adaptation pathways and highlight key tissue types involved in root stress response.

Keywords Mangrove, Date palm, Roots, MALDI-MSI, Salinity, Metabolic pathways

To compensate for their lack of mobility, plants have developed unique mechanisms enabling them to rapidly react to changing environmental conditions, adapting their growth and architecture. Specifically, plants living in the desert need to survive a limited supply of water, elevated temperatures, and soils with poor nutrients and high concentrations of salt. Desert plants have evolved different molecular and physiological mechanisms to tolerate their native environment while maintaining their optimal growth and development. For instance, morphological adaptations of roots and leaves contribute to both water retention and absorption[1,2].

Plant cell wall modifications are an important primary response for the plant to adapt its growth to environmental stresses. For example, drought, heat, and salinity stresses induce remodeling of cell wall components like pectins and arabinoxylan[3]. In response to drought, the cell wall polymer suberin accumulates in the root endodermis of different plant species and contributes to preventing water loss[4]. Remarkably, in some

[1]BESE Division, Plant Cell and Developmental Biology Laboratory, King Abdullah University of Science and Technology, Thuwal, Kingdom of Saudi Arabia. [2]Bruker Daltonics GmbH & Co. KG, Bremen, Germany. [3]Department of Biochemistry and Molecular Biology, University of Southern Denmark, Campusvej 55, Odense 5230, Denmark. [4]BESE Division, BioActives Laboratory, King Abdullah University of Science and Technology, Thuwal, Kingdom of Saudi Arabia. ✉email: Ikram.blilou@kaust.edu.sa

tomato varieties, suberin accumulates in the root exodermis as a mechanism of drought tolerance[5]. In desert species like date palm (*Phoenix dactylifera*), prickly pear (*Opuntia ficus indica*), and agave (*Agave americana*), suberized and/or lignified tissue layers, create an apoplastic barrier to prevent water loss[6–8].

Among the plant species that are known for their resilience and tolerance to salinity and high temperature are Date palms, one of the oldest fruit crops in the world that is mainly cultivated across the Middle East and north of Africa[9], and Mangroves (*Avicennia marina*), predominantly located in the coastlines of (sub) tropical areas around the world[10] where they thrive in hypoxic and saline habitats.

Date palms use various strategies to cope with desert conditions. For example, they produce sclerotic thick leaves with a waxy cuticle to reduce water loss[11]. They also use the remote germination mode, where the developing seedling (including root, shoots, and leaf primordia) stays protected within the cotyledonary petiole[8], to enhance their chances of germinating in the desert. Date palms have also developed a complex root system composed of shallow roots that can absorb water on the surface, as well as deeper roots to reach ground water[2].

Mangroves developed unique strategies to cope with the coastal habitats. They have small leaves with a thick cuticle and fewer stomata to preserve water[12]. They also produce pneumatophores, specialized roots that grow upwards, to allow gaseous exchange when roots are submerged under sea water[13].

Changes in plant architecture occur as readout of changes in metabolic pathways in response to stress conditions. In addition, specialized metabolites play a key role in mitigating stress response[14]. This includes osmoprotectants, compatible solutes that accumulate under stress conditions, protecting the cells from reactive oxygen species (ROS) damage, stabilizing proteins and enzymes, and balancing the turgor pressure without disturbing other metabolic functions[15]. They can be categorized mainly as simple sugars, sugar alcohols, complex sugars, amino acids and derivatives, tertiary amines, and sulfonium compounds[16].

In roots, like any other organ, metabolic changes occur during root growth as well as in response to stresses. While conventional metabolomic approaches are powerful tools to identify molecules from tissue extracts under different physiological conditions[17], the Matrix-assisted laser desorption/ionization mass spectrometry imaging (MALDI—MSI) is emerging as an innovative technology to study the spatial distribution of metabolites in biological samples without the need of labeling or staining[18]. In barley, the use of MALDI–MSI allowed the identification of metabolites that are spatially distributed in different zones within the roots under normal and salt conditions[19]. In grape leaf, MALDI—MSI identified accumulation of sucrose at the infection site of the pathogen *P. viticola*[20] while in *Medicago truncatula*, the use of MALDI—MSI detected differences in metabolite distribution in roots and nodules during symbiosis with the nitrogen-fixing bacteria *Sinorhizobium melilotis*[21].

In this study, we characterized root tissue composition in date palms and mangroves seedlings and determined metabolic pathways and their distribution within root tissues using metabolomics and MALDI—MSI.

Staining of cell wall components showed differences in lignin and suberin deposition in different tissue layers of both date palm and mangrove roots. In date palm roots, suberin and lignin are absent from the meristem and accumulate only in the differentiation zone. In contrast, mangrove roots contain lignin and suberin not only in the differentiation zone but also in the meristem.

Metabolomic analysis revealed differential metabolic pathways in both species. In date palm, we found an enrichment of pathways involved in the biosynthesis or metabolism of amino acids. In the mangrove roots, we detected cell wall components like lignin and suberin, together with amino acids.

Using MALDI-MSI, we revealed distinct spatial distributions of metabolites in cross-sections of date palm and mangrove roots from both meristematic and differentiation zones. In date palm meristems, fatty acids accumulated in the inner and outer cortex, while flavonoids were concentrated in the outermost layers. In mangrove meristems, oraposide, a phenylpropanoid, was found exclusively in the endodermis, while cyclopentapyran, 7-deoxyloganic acid, naphthazarin, and marticin were abundant in the endodermis, epidermis, and exodermis.

The differentiation zone also showed distinct metabolite accumulation and distribution patterns, with phospholipids specific to date palm, while in mangroves, a hydrolysable tannin and a disaccharide distributed across the epidermis/exodermis, cortex, and vasculature. Additionally, osmoprotectants were identified in both species: amino acid-based osmoprotectants were dominant in date palms, while carbohydrate-based (disaccharide) osmoprotectants were prevalent in mangroves. Notably, MALDI-MSI detected palmitic acid, an osmoprotectant unique to date palm, in the inner and outer cortex.

Our study highlights the species- and tissue-specific spatial distribution of metabolites within root zones, offering new insights into the mechanisms underlying salinity, drought, and hypoxia tolerance in contrasting habitats.

Results

Anatomy of date palm and mangrove roots reveals distinct tissue morphology and cell wall composition

To assess the root anatomy in both date palms and mangroves, we analyzed their tissue composition and cell wall components in the meristem within the division zone and in the differentiation zone (Fig. 1A and A' and 2 A) using the recently described triple staining protocol[22]. Calcofluor White (CF) was used to visualize the cell wall, Fluorol Yellow 088 (FY) to detect suberin and Basic Fuchsin (BF) to evaluate lignin deposition.

Date palm and mangrove primary roots have multiple cortex layers, with fiber cells distributed within the cortex of the date palm roots and aerenchyma (in the differentiation/elongation zones) in both mangroves and date palms. The outer tissue layers in date palms, are composed of exodermis surrounded by the rhizodermis/velamen, while in mangroves, they contain the exodermis and epidermis. (Figures 1 and 2 and Supplementary Fig. 1).

Fluorol yellow and basic fuchsin staining of date palm cross-sections from the root meristem showed no accumulation of suberin and lignin within the tissue layers (Fig. 1B-B''' and Supplementary Fig. 1). In contrast,

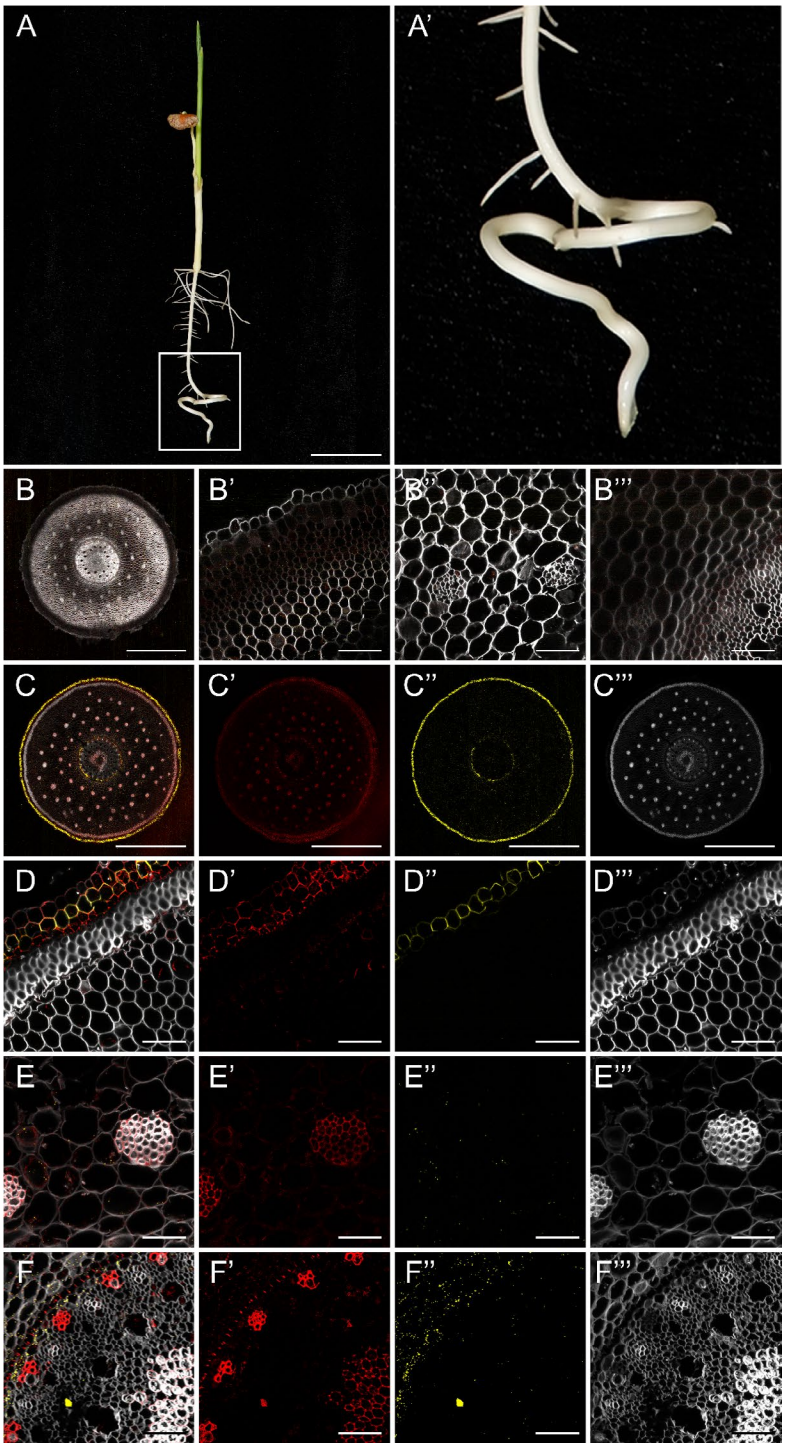

Fig. 1. Date palm seedling and triple staining of cell wall components of date palm roots cross-sections. (**A**) 45 days old date palm seedling. (**A'**) Zoom of the meristem and differentiation zones used in this study. (**B**-**B'''**) Triple staining of meristematic cross-sections. Full cross-section 10x magnification (**B**), exodermis (**B'**), cortex with fibers (**B''**) and cortex, endodermis and vasculature (**B'''**). (**C**-**F'''**) Triple staining of cross-sections from the differentiation zone. (**C**-**C'''**) Full cross-sections 10x magnification. Merged (**C**), Basic Fuchsin (**C'**), Fluorol Yellow (**C''**) and Calcofluor White (**C'''**). (**D**-**D'''**) Rhizodermis/velamen and exodermis. Merged (**D**), Basic Fuchsin (**D'**), Fluorol Yellow (**D''**) and Calcofluor White (**D'''**). (**E**-**E'''**) Cortex with fibers. Merged (**E**), Basic Fuchsin (**E'**), Fluorol Yellow (**E''**) and Calcofluor White (**E'''**). (**F**-**F'''**) Endodermis and vasculature. Merged (**F**), Basic Fuchsin (**F'**), Fluorol Yellow (**F''**) and Calcofluor White (**F'''**). Scale bars: 5 cm (**A**), 1 cm (**A'**), 587.9 µm (**B**), 49.1 µm (**B'**-**B'''**, **D**-**D'''**, **F**-**F'''**), 872.5 µm (**C**-**C'''**), 36.8 µm (**E**-**E'''**). CS: Casparian Strips; diff: differentiation; En: Endodermis; Fi: Fibers; IC: Inner Cortex; me: meristem; OC: Outer Cortex; Ph: Phloem; R/V: Rhizodermis/Velamen; Xy: Xylem.

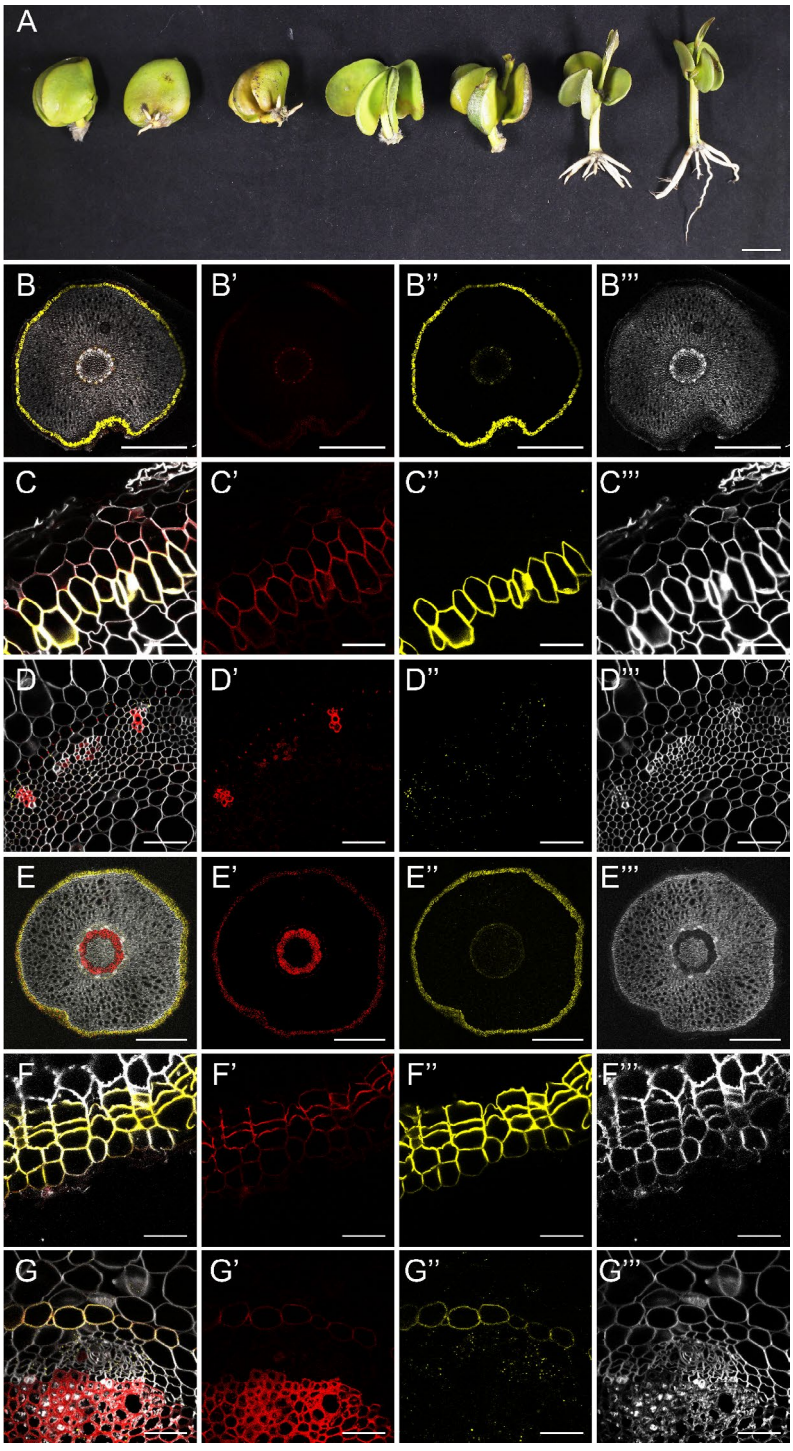

Fig. 2. Mangrove seedlings and triple staining of cell wall components of mangrove roots cross-sections. (**A**) Different stages of mangrove seeds germination. (**B**-**D'''**) Triple staining of meristematic cross-sections. (**B**-**B'''**) Full cross-section 10x magnification. Merged (**B**), Basic Fuchsin (**B'**), Fluorol Yellow (**B''**) and Calcofluor White (**B'''**). (**C**-**C'''**) Epidermis and exodermis. Merged (**C**), Basic Fuchsin (**C'**), Fluorol Yellow (**C''**) and Calcofluor White (**C'''**). (**D**-**D'''**) Endodermis and vasculature. Merged (**D**), Basic Fuchsin (**D'**), Fluorol Yellow (**D''**) and Calcofluor White (**D'''**). (**E**-**G'''**) Triple staining of cross-sections from the differentiation zone. (**E**-**E'''**) Full cross-section 10x magnification. Merged (**E**), Basic Fuchsin (**E'**), Fluorol Yellow (**E''**) and Calcofluor White (**E'''**). (**F**-**F'''**) Epidermis and exodermis. Merged (F), Basic Fuchsin (**F'**), Fluorol Yellow (**F''**) and Calcofluor White (**F'''**). (**G**-**G'''**) Endodermis and vasculature. Merged (**G**), Basic Fuchsin (**G'**), Fluorol Yellow (**F''**) and Calcofluor White (**F'''**). Scale bars: 2 cm (**A**), 869.5 µm (**B**-**B'''**), 36.8 µm (**C**-**C'''**), 49.1 µm (**D**-**D'''**, **F**-**F'''**, **G**-**G'''**), 867.5 µm (**E**-**E'''**). Co: Cortex; CS: Casparian Strips; diff: differentiation; En: Endodermis; Ep: Epidermis; Ex: Exodermis; me: meristem; Pi: Pith; Xy: Xylem.

meristematic cross-sections of mangrove roots have high suberin and lignin with a double layer of lignin present in the epidermis and exodermis and a monolayer of suberin in the exodermis (Fig. 2B and C"). The meristematic endodermis layer in the mangrove accumulates only lignin and no suberin (Fig. 2D-D"), and lignified xylem poles are present in the outer vasculature (Fig. 2D-D").

The differentiation zone of date palm roots shows a lignified rhizodermis/velamen and exodermis. The exodermis also accumulates a monolayer of suberin (Fig. 1D-1D"). The inner cortex has lignified sclerenchyma fibers (Fig. 1C-C'" and 1E-E"). The endodermis, xylem cells, and pith cells contain lignin and no suberin (Fig. 1F-F"). In mangroves, the epidermis has no lignin nor suberin (Fig. 2F). The exodermis, on the other hand, shows four layers containing both polymers (Fig. 2F and F"). The endodermis accumulates both suberin and lignin and the xylem vessels are highly lignified. In the pith, no suberin or lignin are observed (Fig. 2G-G").

Metabolite profiling in date palm and mangrove roots reveals distinct metabolic pathways in both species

To evaluate the differences in the metabolites pool from date palm and mangrove, we extracted the total metabolites from both plants' roots, and these were analyzed by Liquid Chromatography coupled to Mass Spectrometry (LC-MS). The total amount of metabolites detected in both positive and negative ionization modes is shown in Supplementary Table 1. Considering both ion polarities, we identified 1365 metabolites in date palm and 1136 in mangrove root extracts based on their similarities with those deposited in the Compound Discoverer library. From the identified metabolites, 373 were common for both plants (Supplementary Fig. 2).

To investigate which metabolic pathways were enriched in date palm or mangrove, we used the web tool Metaboanalyst 5.0[23]. The top 10 enriched pathways are listed in Supplementary Tables 2 and 3. The significantly enriched metabolic pathways of date palm consist of the biosynthesis of aminoacyl-tRNA and arginine, together with the metabolism of nicotinate and nicotinamide and alanine, aspartate, and glutamate. For mangrove, phenylpropanoid, and cutin, suberin, and wax biosynthesis together with C5-branched dibasic acids and butanoate metabolism are enriched. Six pathways were common for both plants, and they include biosynthesis and/or metabolism of different amino acids (valine, leucine, isoleucine, phenylalanine, tyrosine, and tryptophan), unsaturated fatty acids, isoquinoline alkaloid and monobactam.

MALDI-MSI reveals tissue- and specie-specific distribution of metabolites in the root tissues

To study the spatial distribution of differential metabolites in date palm and mangrove roots, we used MALDI-MSI on cross-sections from the meristem and differentiation zones from date palm and mangrove, where we detected several metabolites between 200 and 1200 m/z.

We performed an untargeted search and manually selected metabolites exclusive to date palm or mangrove roots, as well as those detected in both plant species, and focused on metabolites with a tissue-specific localization pattern.

When comparing the root meristem, we found 45 metabolites unique for date palm (Supplementary Table 4) and 51 for mangrove (Supplementary Table 5). Fifty-three metabolites were common in both plants (Supplementary Table 6). In date palm roots, linoleic acids, and derivatives, together with fatty acids and conjugates, are mostly distributed in the inner and outer cortex (Supplementary Table 4). In the rhizodermis/velamen and exodermis, two flavonoids, one cinnamate ester, and one steroidal glycoside are present (Supplementary Table 4). While we detected metabolites with an accumulation specific to the vasculature and cortex, these could not be identified (Supplementary Fig. 3 and Supplementary Table 4).

In the meristem of mangrove roots, we found oraposide exclusively in the endodermis, while cyclopentapyran, 7-deoxyloganic acid, naphthazarin and marticin were also observed in the endodermis and epidermis/exodermis (Fig. 3C, Supplementary Table 5). The rest of the metabolites detected could not be identified (Fig. 3D, Supplementary Fig. 3B-D and Supplementary Table 5).

Common metabolites observed in the meristem of date palm and mangrove roots are mostly distributed in the epidermis/exodermis of both plants (Supplementary Fig. 4 and Supplementary Table 6). The disaccharides palatinose and trehalose are exclusively in the epidermis/exodermis, while some lipids are found in the epidermis/exodermis and endodermis (Supplementary Fig. 4 and Supplementary Table 6).

We also compared metabolite distribution in the differentiation zone from date palm and mangrove roots. We detected 29 metabolites exclusively in date palm, nine in mangrove and 10 in both species (Supplementary Fig. 5, Supplementary Fig. 6 and Supplementary Tables 7, 8 and 9). Various kinds of phospholipids are specific to date palm, while a hydrolysable tannin and a disaccharide, observed across the epidermis/exodermis, cortex, and vasculature, are unique for mangrove. Of the 10 metabolites in common, only one could be assigned as a disaccharide (melibiose) while the rest remained unidentified (Supplementary Fig. 6 and Supplementary Table 9).

Differential spatial accumulation of osmoprotectants as a read-out for tolerance to challenging habitat

Osmoprotectants are small metabolites that balance osmotic potential in plants when faced with osmotic stress. To evaluate their accumulation and spatial distribution in mangroves and date palms, we conducted a targeted search of osmoprotectants using the list published by Bougouffa et al.[24]. This list compiles 141 metabolites confirmed as osmoprotectants and associates them to reactions, enzymes, genes, or organisms. In the metabolomics data set, we found 22 and 10 exclusive osmoprotectants in date palms and mangroves, respectively, while 14 of these were common in both plants (Supplementary Table 10). Most of the osmoprotectants found in date palms were amino acids (13 out of 22), while in mangroves, they were predominantly carbohydrates (disaccharides, 5 out of 10).

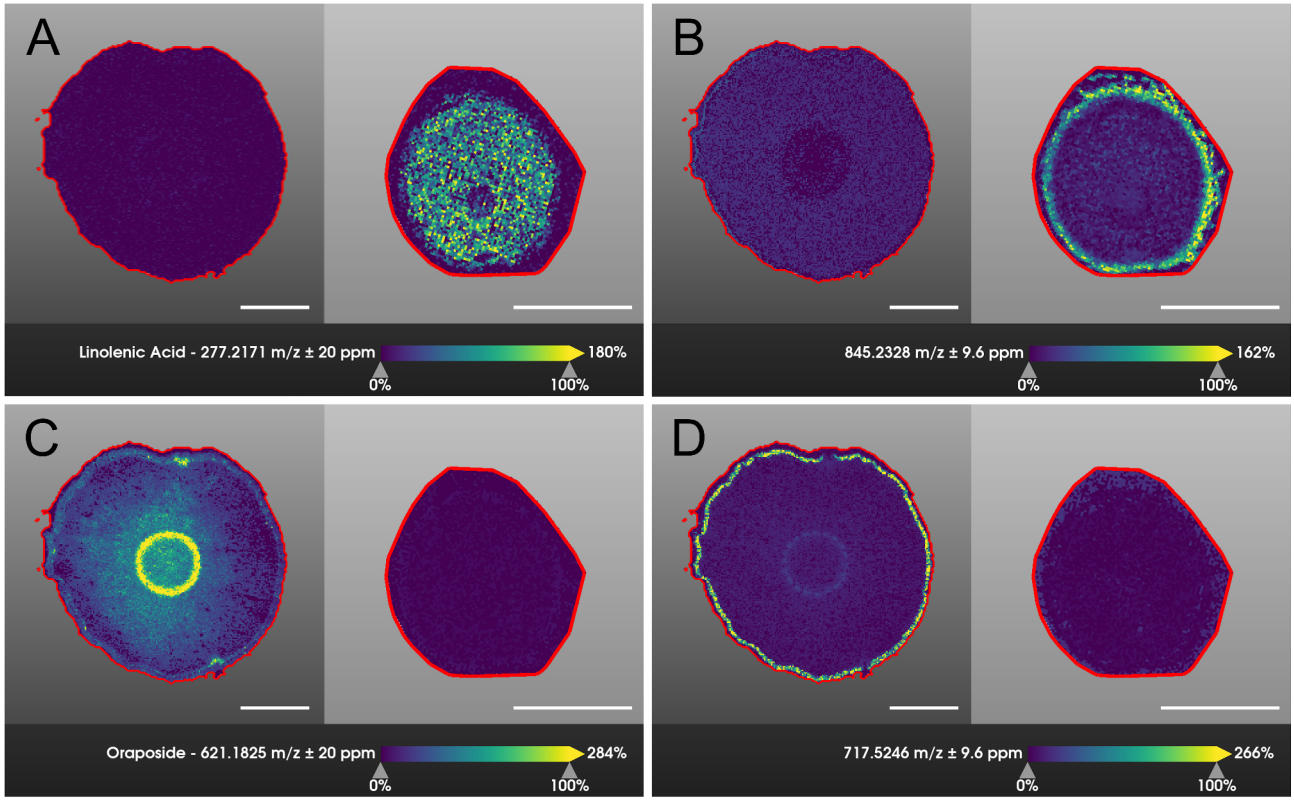

Fig. 3. MALDI-MSI results shown in the SCiLS Lab software. An interval width of ± 9.6ppm and ± 20ppm were chosen to detect and display a single peak of interest within the given interval. The color bar shows a blue color for low intensity and yellow for the highest intensity. A hot spot removal was performed at 99% quantile of all image intensities so that the highest intense last percent was set down to 100%. The color bar is extended by a right-pointing triangle and the maximum intensity found in the image is displayed next to the color bar as a percent value relative to the intensity cut-off. The root meristem cross-sections from date palm and mangrove are shown. Left section: mangrove, Right section: date palm. (**A**) and (**B**) examples of metabolites only detected in date palm cross-sections. Unknowns: 1048.5406 m/z (**A**) and 845.2328 m/z (**B**). (**C**) and (**D**) examples of metabolites only detected in mangrove cross-sections. Oraposide 621.1825 m/z (**C**) and unknown 717.5246 m/z (**D**). Scale bars: 1 mm (**A**-**D**). Co: Cortex; En: Endodermis; Ep: Epidermis; Ex: Exodermis; R/V: Rhizodermis/Velamen.

We ranked them based on their abundance (Fig. 4D and E), where the most abundant osmoprotectants in date palm were trehalose, palmitic acid, choline, malic acid, and fructose, whilst in mangrove, trehalose, maltose, and choline.

We found only four osmoprotectants in the MALDI-MSI data, one exclusively in date palm and three in common for both plants (Fig. 4A, B and C and Supplementary Table 11). Three out of the four metabolites were also detected in the metabolomics results: palatinose, palmitate and trehalose. Palatinose and trehalose are disaccharides, and they are both present in the exodermis/epidermis of date palm and mangrove root meristems. Palmitate is a saturated fatty acid present in plasma membranes. In date palm sections from the root meristem, palmitate is distributed in the inner and outer cortex, but it is not observed in mangrove (Fig. 4).

Discussion

Date palms and mangroves can withstand harsh environmental conditions and thus are good models to study and understand the mechanism of tolerance to high temperatures, salinity, and hypoxia. Their resilience arises not from a single plant feature, but from a series of adaptations at multiple levels. These adaptations involve the rewiring of metabolic pathways, enabling the plants to respond effectively to environmental stresses while maintaining their overall fitness.

Our study highlights common and different developmental and metabolic adaptations of date palms and mangroves that are plausibly contributing to their resilience (Fig. 5).

One adaptive trait in date palm roots that confer tolerance to drought and salinity is the presence of lignin in the outer layers (rhizodermis/velamen and exodermis) and suberin in the exodermis (Fig. 1 and Supplementary Fig. 1). In plants, deposition of hydrophobic barriers has been shown to prevent water loss[25]. For instance, in tomatoes, the accumulation of suberin in the exodermis is required for tolerance to drought[5]. In *Arabidopsis*, prolonged drought and increases salinity levels induce suberin accumulation in the roots[26]. Changes in suberin composition contribute to preventing water loss under high salt and root dehydration when plants are under

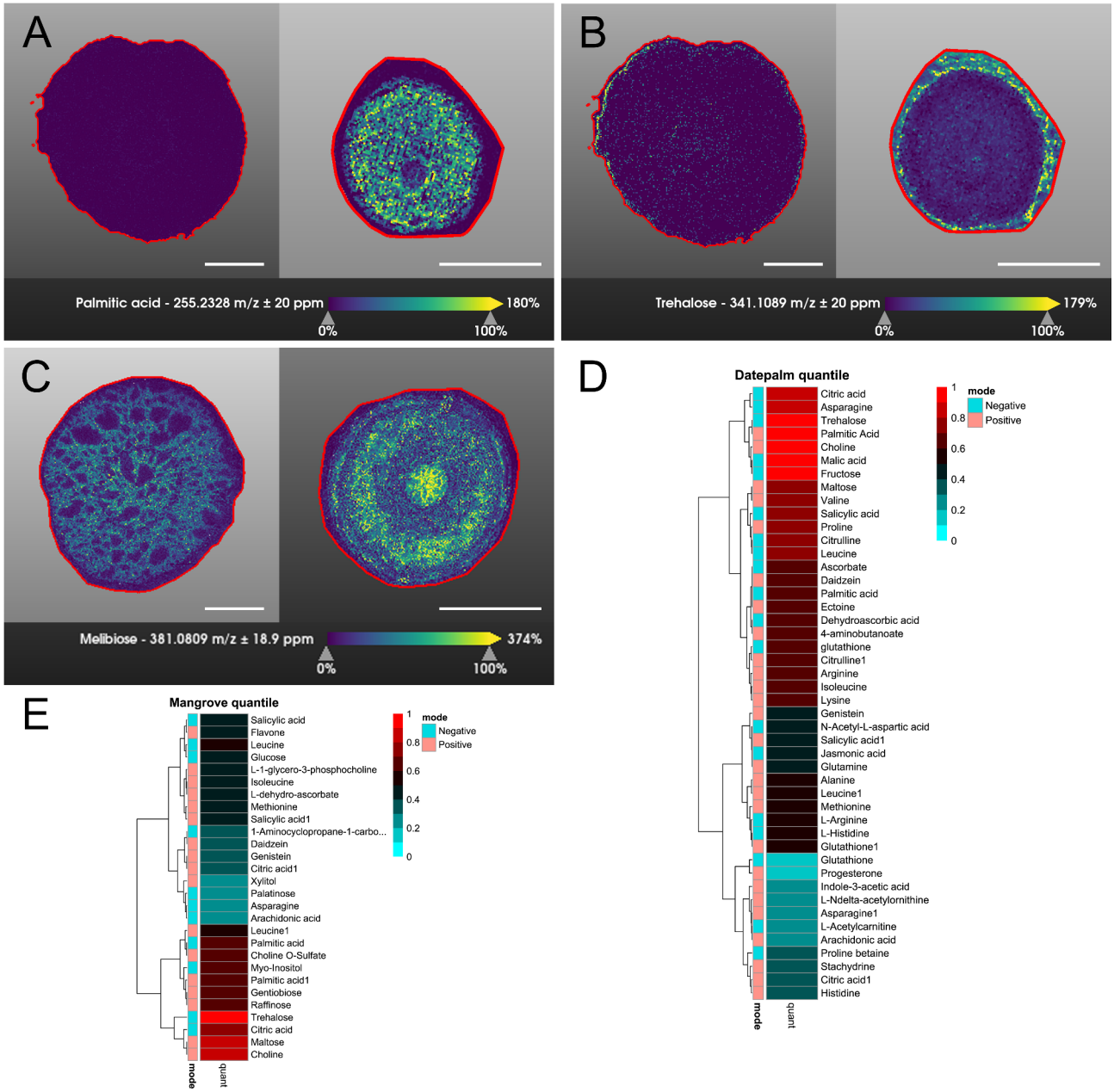

Fig. 4. Osmoprotectants found in date palm and mangrove by MALDI-MSI and metabolomics. (**A**-**C**) Osmoprotectants found by MALDI-MSI and shown in the SCiLS Lab software. (**A**) and (**B**) cross-sections from meristem and (**C**) cross-sections from differentiation. (**A**) Palmitic acid (255.2328 m/z) found only in date palm; (**B**) Trehalose (341.1089 m/z) and (**C**) Melibiose (381.0809 m/z) found in date palm and mangrove. An interval width of ± 18.9ppm and ± 20ppm were chosen to detect and display a single peak of interest within the given interval. The scale bar shows a blue color for low intensity and yellow for the highest intensity. A hot spot removal was performed at 99% so that the intensities were to 100%. The value at the right side of the scale bar shows the percentage value that indicates the proportion of the data that was affected by the hot spot removal process. (**D**-**E**) Heat maps of osmoprotectants found in the metabolomics data in date palm (**D**) and mangrove (**E**). Color represents the relative abundance as percentiles of the distribution of all the metabolites detected in the sample, where 1 would be the most abundant metabolite and 0 the least abundant. Row annotation color indicates the mode of the metabolomics experiment, negative and positive. Scale bars: 1 mm (**A**-**C**). Ae: Aerenchyma; Co: Cortex; E: Exodermis; OC: Outer Cortex; R/V: Rhizodermis/Velamen; Va: Vasculature.

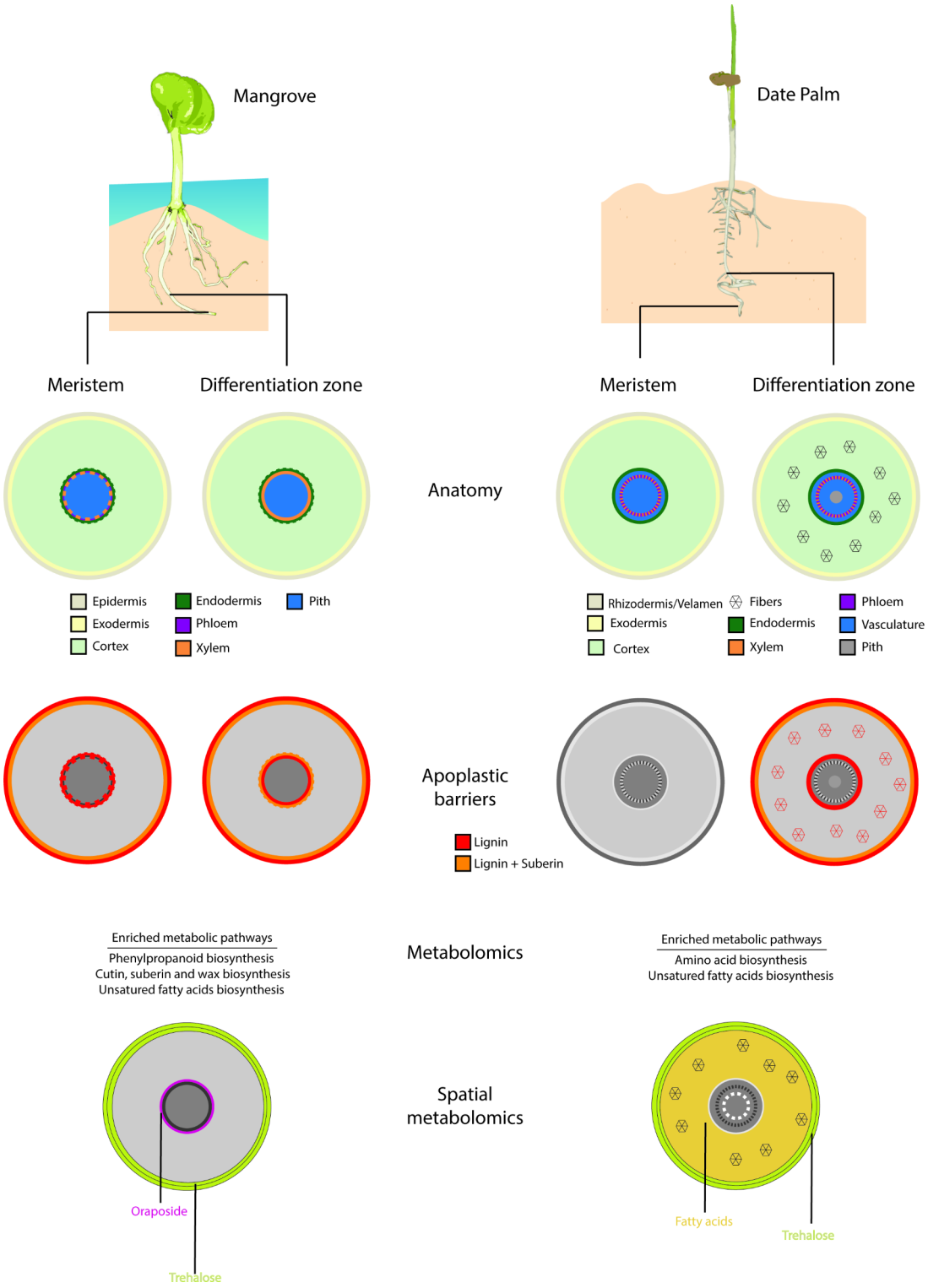

Fig. 5. Schematic presentation illustrating anatomical tissue features in Mangroves and Date palm roots, lignin and suberin accumulation, and tissue-specific metabolites deposition.

drought stress. Plausibly, regulation of suberin accumulation can be considered as a mechanism to alleviate abiotic stress[27]. Furthermore, suberin deposition plays a major role in preventing oxygen loss when roots are subjected to hypoxia (reviewed in[28]). Suberin is also induced in response to biotic stress and can act as a barrier to restrict pathogen invasion and prevent it from entering the vasculature (reviewed in[29]). In tomato for instance, inducing lignin and suberin genes restricts the invasion of the pathogen *R. solanacearum* leading to resistance[30].

The cortex of date palm roots contains fibers made of lignin (Fig. 1E). These fibers provide structural support to the roots[31] and their lignified composition indicates that they might act as a barrier against water loss and might contribute to water transport across the root in date palm. The endodermis accumulates mostly lignin (Fig. 1F), indicating retention and transport of water through the root.

In mangroves, we found an accumulation of suberin and lignin in the meristem (Fig. 2). Unlike most species where lignin and suberin accumulate at the differentiation zone, in mangroves, the epidermis and endodermis contained mostly lignin, while the exodermis had both (Fig. 2). Accumulation of these compounds already in the meristem reflects a robust strategy in mangrove to deal with osmotic stress, due to their continuous exposure to salt in their coastal habitat.

In the differentiation zone, in addition to lignin, suberin also accumulated in the epidermis, exodermis and endodermis. The accumulation of suberin in mangroves might contribute to salt exclusion[32]. In rice, it was shown that hypoxia can induce suberin biosynthesis in the exodermis and endodermis[33,34] in a similar way to what we observed in the mangrove's roots. Suberin's deposition might help in decreasing oxygen losses in the underwater roots. Additionally, suberin and lignin accumulation in the exodermis has been described to help with metal tolerance in mangroves[35].

Lignin deposition was also shown to act as a protective barrier against pathogens, in addition to its microbial activity, many components of lignin biosynthesis accumulate in response to pathogens[36–39]. Being resilient, the spatial accumulation of lignin and suberin in date palm and mangrove root tissues create a protective barrier not only against abiotic stresses but also to prevent invasion and restrict the spread of a wide range of pathogens.

Our metabolomic analysis in whole roots identified exclusive and common metabolites for mangrove and date palm, showing different metabolic pathways that are enriched in each plant species (Supplementary Tables 2 and 3). For example, amino acid pathways are the most common in date palms (Supplementary Table 2). Previous metabolomics analysis of date palm leaves and roots shows an accumulation of amino acids after NaCl treatment[40].

Besides serving as building blocks for proteins, amino acids have been described as important metabolites that accumulate in response to different abiotic stresses[41]. Proline, considered one of the most investigated osmoprotectants, was exclusively enriched in date palms roots. Proline accumulates in various plant species in response to different stresses, including salinity and drought[42], and its main function is to stabilize the proteins and act as a free radical scavenger[43]. The accumulation of proline in date palms has been associated with a response against salinity[40].

In mangroves, we mostly found enrichment of phenylpropanoids, cutin, suberin, and wax biosynthesis-related metabolites. These findings are in agreement with the higher lignin and suberin observed in both the meristematic and differentiation zones of the mangrove roots.

Our metabolomic data also reveals that date palms and mangroves accumulate different osmoprotectants, a common mechanism used for plants to face osmotic stresses[44]. The most common osmoprotectants found exclusively in mangroves correspond to sugars (Supplementary Tables 10 and 11). Sugars play roles in osmotic balance, membrane stabilization, and sugar-sensing systems adjustment[41]. Raffinose and glucose both accumulate in mangrove roots, and their levels have been described to increase under osmotic and drought stresses, helping the plants avoid water losses[42]. Interestingly, it has been described that date palms accumulate mainly amino acids instead of sugar as osmoprotectant metabolites[40], which is consistent with our study. Trehalose is a disaccharide and is one of the main osmoprotectants found in plants[45]. It is highly accumulated in both date palms and mangroves (Figs. 4D and E and 5). Trehalose protects the membranes and proteins but normally is found at low concentrations in plants[41]. Interestingly, we could detect trehalose using MALDI-MSI (Fig. 4), and we found that it accumulates in the outer root layers of both plants, which could aid in protecting the cells from osmotic stress. The differential accumulation of osmoprotectants in date palms and mangroves indicates that these species use different metabolic adjustments to tolerate different kinds of stresses present in their native environment.

The MALDI-TOF-MS technology has previously been used in mangroves for the identification of isolated bacteria[46] and to study the structures of polyflavonoid tannins[47,48], while in date palm it has been utilized to identify lignin oligomers[49] and peptides produced after infestation with red palm weevil[50]. To date, there are no reports of using MALDI-MSI to identify and visualize metabolites at spatial resolution in date palm or mangrove.

MALDI-MSI has been used to detect metabolic changes related to tolerance or resistance against abiotic or biotic stresses. For example, in barley roots subjected to salt stress, changes in phosphatidylcholine were detected by MALDI-MSI[19]. This technique was also used to understand grapevine leaves response to UV-C radiation as well as metabolic changes caused after infection with *Plasmopara viticola*[51].

One of the advantages of using this technique is that it can be extended to study the spatial distribution of metabolites produced in a specific tissue. Our MALDI-MSI in roots from date palms and mangroves identified several metabolites that are accumulated exclusively in each plant. Even though many metabolites were detected, the amount that could be identified was significantly low, which can be explained by the absence of chromatographic separation making the identification of metabolites in non-conventional species more complicated[52]. By MALDI-MSI, we found saturated and unsaturated fatty acids in the cortex of meristematic date palm roots (Supplementary Table 4), like linolenic, palmitic, stearic, and oleic acids. The accumulation of linolenic acid has been reported in salt-tolerant maize[53]. As linolenic acid is an antioxidant[54], it might reduce the damage of membranes produced by ROS in date palm during salt stress. This scavenging is an essential process against the overproduction of ROS and subsequent cell damage[55,56]. Other saturated and unsaturated fatty acids, like palmitic, stearic and oleic acid have also been reported as accumulating in safflower under drought stress[57]. In the date palm exodermis, two flavonoids are observed, procyanidin B1 and B2 (Fig. 3A and B).

The two metabolites identified exclusively in mangrove epidermis/exodermis and endodermis, correspond to 7-Deoxyloganic acid and marticin (Supplementary Table 5). 7-Deoxyloganic acid is an iridoid monoterpene and

it has been described in *Catharanthus roseus* as an intermediate in the biosynthesis of secologanin and further monoterpenoid indole alkaloids, compounds with pharmaceutical properties[58,59]. Marticin is a naphthazarin phytotoxin produced by some *Fusarium spp.* described as a toxic molecule for tomato and pea plants[60]. There is yet no evidence that these compounds are related to abiotic stress tolerance or resistance. Oraposide, a phenylpropanoid compound with antioxidant properties[61] is found to be highly accumulated in the endodermis of mangrove meristematic roots (Fig. 3C). Due to its localization and characteristics, oraposide might help with ROS scavenging in mangrove roots.

Our study provides new insight into the mechanisms of tolerance in resilient species. Using MALDI-MSI, we successfully detected metabolites that have a specific tissue type localization and that might confer a spatial role in stress response within tissues and organs. Introducing new pathways and or manipulating the existing ones in non-resilient species will contribute greatly to target pathways in specific tissues and improve plant tolerance to stresses. Such engineering in plants will require understanding the relevance of the spatial metabolite differences.

We showed that MALDI-MSI has the potential to detect and visualize the distribution of common and unique metabolites, however, many detected metabolites remained unidentified. In addition, the number of metabolites detected by this technology remains low when compared with LC-MS, mainly because by MALDI-MSI, metabolites present only in one specific tissue are studied, as opposed to LC-MS, where the total pool of metabolites present in one organ, i.e., root, are investigated. Advances in increasing sensitivity, as well as combining metabolomics with other emerging omics technologies, such as spatial proteomics, might contribute, at least in part, to overcome these limitations.

Methods

Plant material and root tissue sections

Mangrove seedlings with intact roots were collected from North Beach at King Abdullah University for Science and Technology. One cm root pieces from the meristem and differentiation zone were cut and fixed in 4% paraformaldehyde (PFA) and kept in the dark at 4 °C until sectioning.

Date palm seeds were grown in test tubes containing MS germination medium and once roots and shoots were produced, one cm root pieces from the meristem and differentiation zone were cut and fixed in 4% PFA and kept in the dark at 4 °C until sectioning. Before sectioning, the root material was rinsed twice in Phosphate-buffered saline (PBS) 1X. After washing, the root material was embedded in 10% agarose. 100 µm cross-sections were made with a Vibratome Leica VT 1200 S and stored in Mili-Q water at 4 °C in the dark before staining.

Tissue staining and imaging

Cell wall components were stained following the Triple staining protocol[22]. Briefly, cross-sections were immersed in 0.2% Basic Fuchsin (lignin staining) solution and incubated at room temperature. After 10 min, cross-sections were washed twice with Clearsee and once briefly with MQ-H_2O. Suberin staining was done by incubating the cross-sections in Fluorol Yellow 0.01% for 30 min at room temperature. Finally, cross-sections were immersed in Calcofluor White 0.1% for 15 min for cell wall staining. Cross-sections were rinsed with 50% ethanol and MQ-H_2O and kept at 4 °C until imaging. Confocal imaging was done in a Leica Stellaris 8 confocal using the following settings: for Basic Fuchsin staining, an excitation of 555 nm and emission of 560–730 nm were used; for Fluorol Yellow, an excitation of 488 nm and an emission of 495–560 nm; and for Calcofluor White, an excitation of 405 nm and an emission of 420–480 nm. Sections from date palm and mangrove were imaged using a HC PL FLUOTAR 10x/0.30 DRY and HC PL APO CS2 63x/1.20 WATER objectives.

Metabolite extraction and sample preparation for LC-MS

Fresh date palm and mangrove roots from seedlings were collected in liquid nitrogen and kept at -80 °C before metabolites extraction. Soluble compounds were extracted from 6 different date palm and mangrove roots samples as follows: 50 mg of each sample was mixed with 800 ml 80% methanol and ground at 65 kHz for 90 s, vortexed, and sonicated for 30 min at 4 °C. After 1 h at -20 °C, samples were vortexed for 30 s, moved back at -20 °C for 30 min, and centrifuged for 15 min at 12,000 rpm and 4 °C. 200 ml of each supernatant was mixed with 5 ml of 0.14 mg/ml DL-o-Chlorophenylalanine and transferred to an LC-MS vial. Roots extracts were profiled in both positive and negative ionization modes using the mass spectrometer UltiMate 3000 LC combined with Q Exactive MS (Thermo) and equipped with an ACQUITY UPLC HSS T3 column (100×2.1 mm x 1.8 mm). The mobile phase was composed of solvent A (0.05% formic acid water) and solvent B (acetonitrile), and it was gradually changed as follows: 0–1.0 min, 5% solvent B; 1.0–12 min, 5-95% solvent B; 12.0–13.5 min, 95% solvent B; 13.5–13.6 min, 95%-5% solvent B; 13.6–16.0 min, 5% solvent B. A mobile phase flow rate of 0.3 $mL \times min^{-1}$ was used. The column and sample manager temperatures were set at 40 °C and 4 °C, respectively. Mass spectrometry parameters for ESI + and ESI- modes were as follows: ESI+: Heater Temp 300 °C; Sheath Gas Flow rate, 45arb; Aux Gas Flow Rate, 15arb; Sweep Gas Flow Rate, 1arb; spray voltage, 3.0KV; Capillary Temp, 350 °C; S-Lens RF Level, 30%. ESI-: Heater Temp 300 °C, Sheath Gas Flow rate, 45arb; Aux Gas Flow Rate, 15arb; Sweep Gas Flow Rate, 1arb; spray voltage, 3.2KV; Capillary Temp, 350 °C; S-Lens RF Level, 60%.

Metabolomics data processing and heat map construction

Raw data was imported to Compound Discoverer 3.3 Software (Thermo Fisher Scientific; https://www.thermofisher.com/cl/es/home/industrial/mass-spectrometry/liquid-chromatography-mass-spectrometry-lc-ms/lc-ms-software/multi-omics-data-analysis/compound-discoverer-software.html). To identify the detected metabolites, mass-to-charge ratios (m/z) together with MS1 and MS2 fragmentation patterns were compared with those deposited in the library Compound Discoverer affiliated thermo Q Exactive (Thermo Fisher Scientific). Identified metabolites were used for metabolic pathways analysis. Metabolic pathways were visualized using the web tool

Metaboanalyst 5.0 (https://www.metaboanalyst.ca/), where a Hypergeometric Test was used as the enrichment method, and the *Arabidopsis thaliana* (thale cress) KEGG pathways were used as a reference.

To generate the osmoprotectants heatmaps, the metabolomics datasets were loaded into R Statistical Software 4.4.2 (https://www.r-project.org/). Negative and positive modes were processed independently. An empirical cumulative distribution function was calculated using the function *ecdf* from the *stats* package; using the average of the peak areas of the three replicates corresponding to all metabolites detected in the assay. This function was used to calculate the proportion of observations in the data that are less than or equal to the metabolites displayed in the heatmaps.

Root tissue cryosectioning and sample preparation for MALDI-MSI

Root samples from the meristem and differentiation zones of approximately 1 cm in length were harvested from date palm seedlings grown in pots and mangrove seedlings collected from KAUST North Beach. Roots were embedded either in 5% gelatin or using a 2-hydroxyethyl cellulose (HEC, 1%). Both embedding media were cooled to room temperature before they began to harden to avoid breaks. A small piece of root tissue was placed in a plastic mold containing the corresponding embedding medium and then transferred onto dry ice until the sample and medium solidified. The solidified blocks were sectioned at a thickness of 12 µm using a Leica CM1950 Cryostat (Leica, Wetzlar, Germany). Tissue sections were mounted onto Bruker's IntelliSlides, cold-dried under vacuum, and stored for future MALDI-MSI experiments. A DHAP (Dihydroxyacetone phosphate, Bruker Daltonics, Bremen, Germany) matrix solution was prepared and applied to the plant sections using a HTX sprayer M3 (HTX Technologies LLC, Carrboro, USA) following the Bruker standard protocol to ensure consistent and uniform matrix coverage.

MALDI-MSI

Data acquisition was conducted on a timsTOF fleX MALDI-2 mass spectrometer (Bruker; https://www.bruker.com/en/products-and-solutions/mass-spectrometry/timstof/timstof-flex.html) with the Trapped Ion Mobility Spectrometry (TIMS) mode enabled. The Smartbeam 3D laser was set to operate at a repetition rate of 1 kHz in MALDI-2 mode. Negative ion polarity was used with a mass range of 200–1200 m/z. TIMS parameters included a 200 ms ramp time within a 1/K0 range of 0.6 to 1.8 $V{\cdot}s/cm^2$. To achieve high spatial resolution, a raster width of 20 µm was employed. The same settings were chosen for measurements in positive ion mode.

Raw data was imported to SCiLS Lab 2023a software (Bruker; https://www.bruker.com/en/products-and-solutions/mass-spectrometry/ms-software/scils-lab.html) for metabolites visualization. For metabolite annotation, the MetaboScape 2023b software (Bruker; https://www.bruker.com/en/products-and-solutions/mass-spectrometry/ms-software/metaboscape.html) and a target list generated out of the LC-MS/MS data were used. Those metabolites observed in the vasculature, endodermis, cortex, exodermis, and/or epidermis were selected manually out of annotated features.

Data availability

The datasets used and/or analysed during the current study are available from the corresponding author upon reasonable request.

Received: 17 November 2024; Accepted: 2 January 2025
Published online: 07 January 2025

References

1. Bano, C., Amist, N. & Singh, N. B. Morphological and anatomical modifications of plants for environmental stresses. *Mol. Plant. Abiotic Stress: Biology Biotechnol.* 29–44 (2019).
2. Kirschner, G. K., Xiao, T. T. & Blilou, I. Rooting in the desert: a developmental overview on desert plants. *Genes (Basel).* **12**, 709 (2021).
3. Tenhaken, R. Cell wall remodeling under abiotic stress. *Front. Plant. Sci.* **5**, (2015).
4. Zhang, L. et al. Drought activates MYB41 orthologs and induces suberization of grapevine fine roots. *Plant. Direct.* **4**, e00278 (2020).
5. Cantó-Pastor, A. et al. A suberized exodermis is required for tomato drought tolerance. *Nat. Plants.* **10**, 118–130 (2024).
6. NORTH, G. B. & NOBEL, P. S. Radial hydraulic conductivity of individual Root tissues ofOpuntia ficus-indica (L.) Miller as Soil moisture varies. *Ann. Bot.* **77**, 133–142 (1996).
7. Kauff, F., Rudall, P. J. & Conran, J. G. Systematic root anatomy of Asparagales and other monocotyledons. *Plant Syst. Evol.* **223**, 139–154 (2000).
8. Xiao, T. T. et al. Emergent protective organogenesis in date palms: a morpho-devo-dynamic adaptive strategy during early development. *Plant. Cell.* **31**, 1751–1766 (2019).
9. Jaradat, A. A. & Biodiversity Genetic diversity, and genetic resources of date palm. in Date Palm Genetic Resources and Utilization: Volume 1: Africa and the Americas (eds Al-Khayri, J. M., Jain, S. M. & Johnson, D.) V) 19–71 (Springer Netherlands, Dordrecht, doi:https://doi.org/10.1007/978-94-017-9694-1_2. (2015).
10. Nagelkerken, I. et al. The habitat function of mangroves for terrestrial and marine fauna: a review. *Aquat. Bot.* **89**, 155–185 (2008).
11. Du, B. et al. How to cope with stress in the Desert—the date Palm Approach. *Plant. Cell. Environ.* (2024).
12. Naskar, S. & Palit, P. K. Anatomical and physiological adaptations of mangroves. *Wetl Ecol. Manag.* **23**, 357–370 (2015).
13. Srikanth, S., Lum, S. K. Y. & Chen, Z. Mangrove root: adaptations and ecological importance. *Trees* **30**, 451–465 (2016).
14. Wu, M., Northen, T. R. & Ding, Y. Stressing the importance of plant specialized metabolites: omics-based approaches for discovering specialized metabolism in plant stress responses. *Front. Plant. Sci.* **14**, 1272363 (2023).
15. Singh, M., Kumar, J., Singh, S., Singh, V. P. & Prasad, S. M. Roles of osmoprotectants in improving salinity and drought tolerance in plants: a review. *Rev. Environ. Sci. Biotechnol.* **14**, 407–426 (2015).
16. Majumder, A. L., Sengupta, S. & Goswami, L. Osmolyte Regulation in Abiotic Stress. in Abiotic Stress Adaptation in Plants: Physiological, Molecular and Genomic Foundation (eds Pareek, A., Sopory, S. K. & Bohnert, H. J.) 349–370 (Springer Netherlands, Dordrecht, doi:https://doi.org/10.1007/978-90-481-3112-9_16. (2010).

17. Manickam, S. et al. Plant Metabolomics: Current Initiatives and Future Prospects. *Current Issues in Molecular Biology* vol. 45 8894–8906 Preprint at (2023). https://doi.org/10.3390/cimb45110558
18. Wittek, O., Jahreis, B. & Römpp, A. MALDI MS Imaging of Chickpea Seeds (Cicer arietinum) and crab's Eye Vine (Abrus precatorius) after tryptic digestion allows spatially resolved identification of Plant proteins. *Anal. Chem.* **95**, 14972–14980 (2023).
19. Sarabia, L. D. et al. High-mass-resolution MALDI mass spectrometry imaging reveals detailed spatial distribution of metabolites and lipids in roots of barley seedlings in response to salinity stress. *Metabolomics* **14**, 1–16 (2018).
20. Maia, M. et al. Grapevine leaf MALDI-MS imaging reveals the localisation of a putatively identified sucrose metabolite associated to Plasmopara viticola development. *Front. Plant. Sci.* **13**, 1012636 (2022).
21. Ye, H. et al. MALDI mass spectrometry-assisted molecular imaging of metabolites during nitrogen fixation in the M edicago truncatula–S inorhizobium meliloti symbiosis. *Plant J.* **75**, 130–145 (2013).
22. Sexauer, M., Shen, D., Schön, M., Andersen, T. G. & Markmann, K. Visualizing polymeric components that define distinct root barriers across plant lineages. *Dev. (Cambridge)* **148**, (2021).
23. Pang, Z. et al. MetaboAnalyst 5.0: narrowing the gap between raw spectra and functional insights. *Nucleic Acids Res.* **49**, W388–W396 (2021).
24. Bougouffa, S., Radovanovic, A., Essack, M. & Bajic, V. B. DEOP: A database on osmoprotectants and associated pathways. *Database* 1–13 (2014). (2014).
25. Liu, T. & Kreszies, T. The exodermis: a forgotten but promising apoplastic barrier. *J. Plant. Physiol.* **154118** (2023).
26. de Silva, N. D. G. et al. Root suberin plays important roles in reducing water loss and sodium uptake in Arabidopsis thaliana. *Metabolites* **11**, 735 (2021).
27. Barberon, M. et al. Adaptation of root function by nutrient-induced plasticity of endodermal differentiation. *Cell* **164**, 447–459 (2016).
28. Kreszies, T., Schreiber, L. & Ranathunge, K. Suberized transport barriers in Arabidopsis, barley and rice roots: from the model plant to crop species. *J. Plant. Physiol.* **227**, 75–83 (2018).
29. Molina, A. et al. Plant cell wall-mediated disease resistance: current understanding and future perspectives. *Mol. Plant.* (2024).
30. Kashyap, A. et al. Induced Ligno-suberin vascular coating and tyramine-derived hydroxycinnamic acid amides restrict Ralstonia solanacearum colonization in resistant tomato. *New Phytol.* **234**, 1411–1429 (2022).
31. Bokor, B. et al. Silicon uptake and localisation in date palm (Phoenix dactylifera)–A unique association with sclerenchyma. *Front. Plant. Sci.* **10**, 988 (2019).
32. Krishnamurthy, P. et al. Role of root hydrophobic barriers in salt exclusion of a mangrove plant Avicennia Officinalis. *Plant. Cell. Environ.* **37**, 1656–1671 (2014).
33. Kotula, L., Ranathunge, K., Schreiber, L. & Steudle, E. Functional and chemical comparison of apoplastic barriers to radial oxygen loss in roots of rice (Oryza sativa L.) grown in aerated or deoxygenated solution. *J. Exp. Bot.* **60**, 2155–2167 (2009).
34. Ranathunge, K., Lin, J., Steudle, E. & Schreiber, L. Stagnant deoxygenated growth enhances root suberization and lignifications, but differentially affects water and NaCl permeabilities in rice (Oryza sativa L.) roots. *Plant. Cell. Environ.* **34**, 1223–1240 (2011).
35. Cheng, H. et al. Metal (pb, zn and cu) uptake and tolerance by mangroves in relation to root anatomy and lignification/suberization. *Tree Physiol.* **34**, (2014).
36. Barber, M. S., McConnell, V. S. & DeCaux, B. S. Antimicrobial intermediates of the general phenylpropanoid and lignin specific pathways. *Phytochemistry* **54**, 53–56 (2000).
37. Eynck, C., Séguin-Swartz, G., Clarke, W. E. & Parkin, I. A. P. Monolignol biosynthesis is associated with resistance to Sclerotinia sclerotiorum in Camelina sativa. *Mol. Plant. Pathol.* **13**, 887–899 (2012).
38. Wuyts, N., Lognay, G., Swennen, R. & De Waele, D. Nematode infection and reproduction in transgenic and mutant Arabidopsis and tobacco with an altered phenylpropanoid metabolism. *J. Exp. Bot.* **57**, 2825–2835 (2006).
39. Cesarino, I. Structural features and regulation of lignin deposited upon biotic and abiotic stresses. *Curr. Opin. Biotechnol.* **56**, 209–214 (2019).
40. Mueller, H. M. et al. Integrative multi-omics analyses of date palm (Phoenix dactylifera) roots and leaves reveal how the halophyte land plant copes with sea water. *Plant. Genome.* **17**, e20372 (2024).
41. Mehta, D. & Vyas, S. Comparative bio-accumulation of osmoprotectants in saline stress tolerating plants: a review. *Plant. Stress.* **9**, 100177 (2023).
42. Jiménez-Arias, D. et al. A beginner's guide to osmoprotection by biostimulants. *Plants* **10**, 363 (2021).
43. Khan, M. S., Ahmad, D. & Khan, M. A. Utilization of genes encoding osmoprotectants in transgenic plants for enhanced abiotic stress tolerance. *Electron. J. Biotechnol.* **18**, 257–266 (2015).
44. Tuteja, N. & Singh, G. S. *Plant Acclimation to Environmental Stress* (Springer Science & Business Media, 2012).
45. Iturriaga, G., Suárez, R. & Nova-Franco, B. Trehalose metabolism: from osmoprotection to signaling. *Int. J. Mol. Sci.* **10**, 3793–3810 (2009).
46. Farhat, T. M., Disi, A., Ashfaq, Z. A., Zouari, N. & M. Y. & Study of diversity of mineral-forming bacteria in Sabkha mats and sediments of mangrove forest in Qatar. *Biotechnol. Rep.* **39**, e00811 (2023).
47. Zhang, L. L., Wang, Y. M., Wu, D. M., Xu, M. & Chen, J. H. Study on the structure of mangrove polyflavonoid tannins with MALDI-TOF Mass Spectrometry and NMR. *Adv. Mat. Res.* **554**, 1988–1993 (2012).
48. Lang, T. et al. How extraction and purification affect MALDI-TOF MS characterization of Mangrove Condensed tannins, an ecologically important secondary metabolites in Coastal Wetland Ecosystem. *Sustainability* **14**, 14960 (2022).
49. Albishi, T. et al. Top-down lignomic matrix-assisted laser desorption/ionization time-of-flight tandem mass spectrometry analysis of lignin oligomers extracted from date palm wood. *Rapid Commun. Mass Spectrom.* **33**, 539–560 (2019).
50. Rasool, K. G. et al. Identification of proteins modulated in the date palm stem infested with red palm weevil (Rhynchophorus Ferrugineus Oliv.) Using two dimensional differential gel electrophoresis and mass spectrometry. *Int. J. Mol. Sci.* **16**, 19326–19346 (2015).
51. Becker, L., Carré, V., Poutaraud, A., Merdinoglu, D. & Chaimbault, P. MALDI mass spectrometry imaging for the simultaneous location of resveratrol, pterostilbene and viniferins on grapevine leaves. *Molecules* **19**, 10587–10600 (2014).
52. Dong, Y., Li, B. & Aharoni, A. More than pictures: when MS Imaging meets histology. *Trends Plant. Sci.* **21**, 686–698 (2016).
53. Gogna, M. & Bhatla, S. C. Salt-tolerant and-sensitive seedlings exhibit noteworthy differences in lipolytic events in response to salt stress. *Plant. Signal. Behav.* **15**, 1737451 (2020).
54. Zi, X., Zhou, S. & Wu, B. Alpha-linolenic acid mediates diverse drought responses in maize (Zea mays L.) at seedling and flowering stages. *Molecules* **27**, 771 (2022).
55. Zhang, X. et al. Combining transcriptome and metabolome analyses to reveal the response of maize roots to pb stress. *Plant Physiol. Biochem.* **109265** (2024).
56. Zhang, M., Smith, J. A. C., Harberd, N. P. & Jiang, C. The regulatory roles of ethylene and reactive oxygen species (ROS) in plant salt stress responses. *Plant. Mol. Biol.* **91**, 651–659 (2016).
57. Joshan, Y., Sani, B., Jabbari, H., Mozafari, H. & Moaveni, P. Effect of drought stress on oil content and fatty acids composition of some safflower genotypes. (2019).
58. Miettinen, K. et al. The seco-iridoid pathway from Catharanthus roseus. *Nat. Commun.* **5**, 3606 (2014).
59. Asada, K. et al. A 7-deoxyloganetic acid glucosyltransferase contributes a key step in secologanin biosynthesis in Madagascar periwinkle. *Plant. Cell.* **25**, 4123–4134 (2013).

60. Pillay, A., Rousseau, A. L. & Fernandes, M. A. De Koning, C. B. Wacker oxidation methodology for the synthesis of the benzo-fused acetal core of marticin. *Tetrahedron* **68**, 7116–7121 (2012).
61. Marti-Mestres, G. et al. The in vitro percutaneous penetration of three antioxidant compounds. *Int. J. Pharm.* **331**, 139–144 (2007).

Acknowledgements
The authors gratefully acknowledge the KAUST Analytical Chemistry Core Lab facility and staff for their support and assistance in this work.

Author contributions
I.B. conceptualized the research and helped with the experimental design. P.O. performed tissue histology, analyzed the metabolomics and MALDI images. T.T.X. performed cryosectioning of date palms and mangroves. J.K.G.K., J.Y.W. and S.B. performed metabolite analysis. T.T.X., C.H., and S.F.F. performed MALDI-MS. P.O. and W.S. performed confocal imaging and staining.P.O. and I.B. wrote the paper. All authors contributed to data analysis and manuscript discussion.

Funding
This work has been supported by King Abdullah University of Science and Technology (KAUST) baseline (BAS/1/1081-01-01).

Declarations

Competing interests
The authors declare no competing interests.

Additional information
Supplementary Information The online version contains supplementary material available at https://doi.org/10.1038/s41598-025-85416-1.

Correspondence and requests for materials should be addressed to I.B.